Nanoscale

RSCPublishing

COMMUNICATION

Current self-complianced and self-rectifying resistive switching in Ag-electroded single Na-doped ZnO nanowires†

Cite this: *Nanoscale*, 2013, **5**, 2651

Received 3rd January 2013
Accepted 13th February 2013

DOI: 10.1039/c3nr00027c

www.rsc.org/nanoscale

Jing Qi,*[a] Jian Huang,[b] Dennis Paul,[c] Jingjian Ren,[b] Sheng Chu[b] and Jianlin Liu*[b]

We demonstrate current self-complianced and self-rectifying bipolar resistive switching in an Ag-electroded Na-doped ZnO nanowire device. The resistive switching is controlled by the formation and rupture of an Ag nanoisland chain on the surface along the Na-doped ZnO nanowire. Na-doping plays important roles in both the self-compliance and self-rectifying properties.

Resistive switching memory (RSM) has been reported as a prominent candidate of the next-generation nonvolatile memory because of its simple structure, high-density integration, low power consumption, fast operation and strong potential for multilevel-per-cell memories.[1–4] Recently, nanoscale RSM has also been linked to the reconfigurable logic applications[5,6] and the concept of memristors[7–9] for analogue circuit[10] and neuromorphic computing[11–13] applications. It is generally believed that the crossbar resistive memory array will yield the most cost-effective solid-state memory. However, each memory cell needs a diode to avoid the misreading caused by the sneak current, especially for bipolar resistive switching, in which a more complicated Zener diode simultaneously satisfying several crucial requirements is needed for each cell.[14] This situation presents extra challenges for the development of 1D1R-based bipolar resistive memory arrays, especially in a 3-dimensional multi-layer stack. Furthermore, a current compliance is indispensable to prevent RSM from hard breakdown.[15] In this letter, we report current self-rectifying and self-complianced resistive switching in a single Na-doped ZnO nanowire. The current self-rectification can provide a solution to suppress sneak current in crossbar arrays,[16] while self-compliance can prevent RSM from hard breakdown.

Na-doped and undoped ZnO nanowires were grown in a quartz tube furnace system. Zinc powder mixed with or without sodium acetate powder in a quartz bottle was placed in the center of the quartz tube. A Si (100) substrate with 10 nm gold catalyst on top was kept 2 cm away from the source on the downstream side. Nitrogen gas with a flow rate of 1000 sccm passed continuously through the furnace. The source and substrate were then heated to a growth temperature of 540 °C. During the growth, a mixture of argon–oxygen (99.5 : 0.5) of 300 sccm was introduced into the quartz tube for ZnO nanowire growth. The growth lasted for 30 min. The microstructure, composition and crystallinity of nanowires were evaluated by scanning electron microscopy (SEM), high resolution transmission electron microscopy (HRTEM) and secondary ion mass spectroscopy (SIMS). The single-nanowire devices were utilized to evaluate the electrical characteristics, which were fabricated on an n-type silicon substrate capped with a thermally oxidized SiO_2 layer of 300 nm. To fabricate the memory device, ZnO nanowires were firstly transferred onto the substrate. Then a standard photolithography process was utilized to pattern the substrate with ZnO nanowires on top, followed by deposition of 100 nm Ag. Electrical characterization was performed in air at room temperature using a semiconductor parameter analyzer (Agilent 4155C). The transportation of Ag during electrical characterization was confirmed by the mapping of Ag utilizing high spatial resolution Auger electron spectroscopy (HSR-AES). The HSR-AES data were acquired with a PHI 700Xi system utilizing a 20 kV 10 nm electron beam.

Fig. 1(a) shows a top view SEM image of the as-grown Na-doped ZnO nanowires. The nanowires do not grow vertically on substrates like undoped ZnO nanowires (see Fig. S1 for SEM images†) because of Na doping. The inset shows the SIMS result, which indicates that Na was doped into the ZnO nanowires. Fig. 1(b) and its inset display a low magnification TEM image of an individual Na-doped ZnO nanowire and its selected area electron diffraction (SAED) pattern, respectively, showing

[a]The Key Laboratory for Magnetism and Magnetic Materials of MOE, Department of Physics, School of Physical Science and Technology, Lanzhou University, Lanzhou, 730000, China. E-mail: qijing@lzu.edu.cn

[b]Quantum Structures Laboratory, Department of Electrical Engineering, University of California, Riverside, California, 92521, USA. E-mail: jianlin@ee.ucr.edu

[c]Physical Electronics, 18725 Lake Drive East, Chanhassen, MN 55317, USA

† Electronic supplementary information (ESI) available. See DOI: 10.1039/c3nr00027c

This journal is © The Royal Society of Chemistry 2013

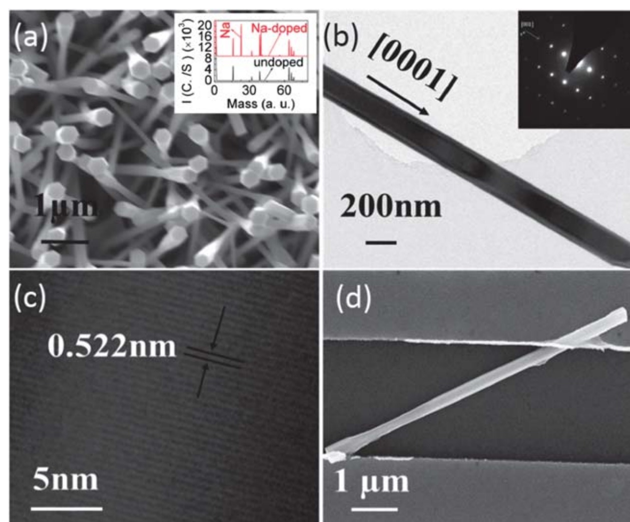

Fig. 1 (a) SEM image and SIMS spectra (inset) of Na-doped ZnO nanowires. Na was doped into ZnO nanowires, which do not grow vertically on the substrate because of doping. (b) TEM image of a Na-doped ZnO nanowire, inset: SAED pattern of the nanowire. The Na-doped ZnO nanowire grows along the [0001] direction. (c) HRTEM image of the nanowire in (b). The change of lattice parameters induced by Na-doping is under the resolution of HRTEM. (d) SEM image of the Na-doped ZnO nanowire resistive switching device. The symmetric structure of Ag/nanowire/Ag was used to simplify the fabrication process.

that the Na-doped ZnO nanowire grows along the [0001] direction. The representative HRTEM image is shown in Fig. 1(c), in which a typical single crystalline ZnO structure could be clearly observed, showing that the change of lattice constant by Na doping is below the resolution of HRTEM. Fig. 1(d) shows an SEM image of the Ag/Na-doped ZnO nanowire/Ag memory device, in which two Ag active electrodes are used, simplifying the fabrication procedure greatly in contrast to the process using one active electrode and one inert electrode.

Fig. 2(a) and (b) show typical *I–V* characteristics of the Na-doped ZnO nanowire device and undoped ZnO nanowire device, respectively. The Na-doped ZnO nanowire device shows bipolar resistive switching set and reset at 40 V and −40 V respectively, which has the self-compliance property with current around 10 μA and self-rectifying property with a rectifying ratio of 10^5 at the low resistance state (LRS). The undoped ZnO nanowire device shows typical bipolar resistive switching, which needs external current compliance and is similar to the results reported by Yang *et al.* in a single crystalline ZnO nanowire electroded by Ag.[17] These results indicate that Na-doping plays important roles in both the self-compliance and self-rectifying properties at LRS. Fig. 2(c) and (d) show retention and DC sweeping endurance characteristics of an Na-doped ZnO nanowire device, respectively. The LRS exhibits no significant degradation after 1×10^5 s, while the high resistance state (HRS) shows no degradation. The two states can still be well distinguished by a high resistance ratio of over 10^3, as the data trends are extrapolated to 10 years. For endurance, as shown in Fig. 2(d), no significant degradation of both LRS and HRS with a large resistance window of over 10^3 can be observed.

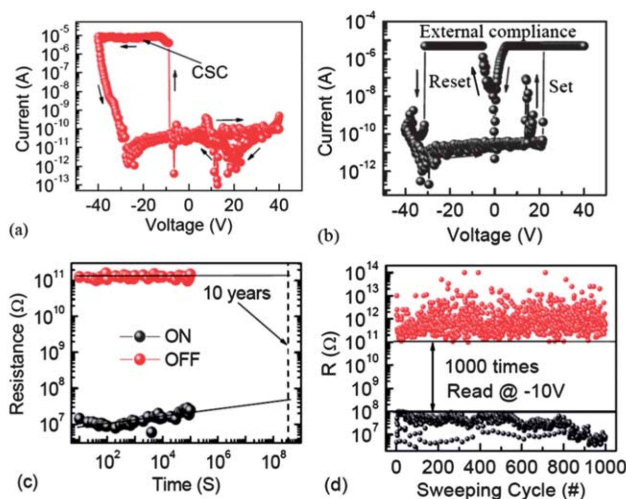

Fig. 2 (a) Typical I–V characteristics of an Na-doped ZnO nanowire device, which shows current self-complianced (CSC) and self-rectified resistive switching behavior set and reset at 40 V and −40 V, respectively. The self-complianced current is about 10 μA and the self-rectifying ratio is 10^5 at the low resistive state. (b) Typical non-rectifying I–V characteristics of an undoped ZnO nanowire device, which needs external compliance. The current self-complianced and self-rectifying properties are due to Na-doping. (c) Retention and (d) endurance results of resistive switching memory fabricated with a Na-doped ZnO nanowire. The two states can still be well distinguished by a high resistance ratio of over 10^3, as the data trends are extrapolated to 10 years. Both the LRS and HRS with a large resistance window during DC sweeping periods of over 10^3 exhibited little degradation.

After electrical measurements, some white dots were found on the biased side of the nanowire as shown in the SEM image in Fig. 3(a), compared with its SEM image before electrical measurements shown in Fig. 1(d). Fig. 3(b) shows the corresponding results of the HSR-AES Ag map after a layer of 1 nm was sputtered away to avoid contamination. Combining Zn and

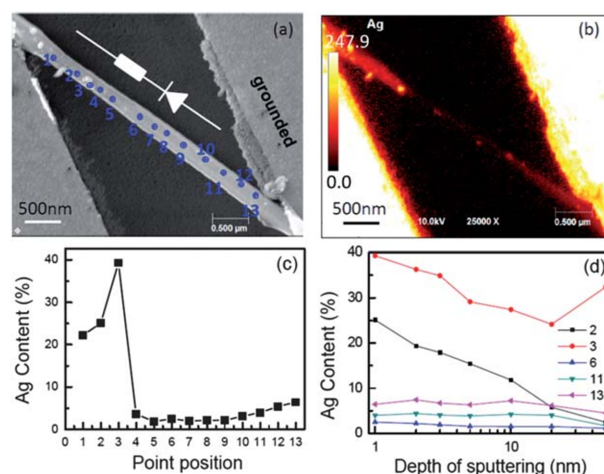

Fig. 3 (a) SEM image and (b) Ag map for the ZnO nanowire resistive switching device. After I–V characterizations, Ag dots show up on the surface of the Na-doped ZnO nanowire. Ag contents along the Na-doped nanowire after I–V characteristics (c) on the surface and (d) after layers with different thicknesses were sputtered away. Ag distributes mainly on the surface of the biased side of the Na-doped ZnO nanowire.

 This journal is © The Royal Society of Chemistry 2013

O maps shown in Fig. S2,† it is concluded that these white dots are composed of Ag. In addition to these white dots, Ag is also distributed along the whole nanowire. The part with the highest Ag content is at the biased end of the nanowire while the lowest one is in the middle. The content of Ag was measured quantitatively choosing 13 points along the nanowire. The results are provided in Fig. 3(c), which shows that the Ag content at the biased end is much higher than that at the grounded end and the middle. The quantitative contents of Ag were also measured for these 13 points after layers of 2 nm, 3 nm, 5 nm, 10 nm, 20 nm, and 50 nm were sputtered away. Fig. 3(d) shows the results. Together with the SEM image and Zn, O, and Ag maps shown in Fig. S3† in the ESI, it indicates that although there are some Ag atoms in the core of the Na-doped ZnO nanowire, Ag is mainly distributed on the surface of the nanowire. While for the nanowire without going through electrical characterization, there is no Ag signal along the whole nanowire, as shown in Fig. S4.† According to Fig. 1(d), 3 and S4,† Ag atoms were transferred onto the ZnO nanowire during *I–V* characterization. These results indicate that the resistive switching in a single Na-doped ZnO nanowire is induced by the formation and rupture of an Ag nanoisland chain on the nanowire surface, as observed by Yang *et al.* in SiO_2-based resistive switching,[18] which is similar to the mechanism reported by Yang *et al.*[17]

The random distribution of Na dopants can serve as a load resistor in series to constrain the current.[19] The Ag mobile ions forming the conducting nanoisland chain can be partially retracted from the grounded side of the nanowire surface at small negative biases which suppresses the device conductance and induces the load resistor to be variable with the increase of negative bias, which corresponds to the self-compliance behavior. The partial retraction of Ag was also observed in the Ag/a-Si/poly-Si system.[20] The self-rectifying behavior of ZnO nanowires can be explained by the asymmetric contacts between ZnO nanowires and Ag electrodes, as reported previously in the structures of Ag/randomly oriented nanorods/Ag,[21] Au/aligned nanorods/Au,[22] and Au/single nanobelt/Au.[23] In Fig. 2(a), the first voltage sweeping process is from 0 V to 40 V, the *I–V* characteristics of which are similar to a diode with the p-type end grounded. When the first voltage sweeping process is from 0 V to −40 V, the *I–V* characteristics are similar to a diode with the n-type side grounded, as shown in Fig. S5.† These results indicate that the direction of the diode is related to the first voltage sweeping process. While in an undoped ZnO nanowire, the *I*–V characteristics show no difference using different first voltage sweeps. Because Na is a p-type dopant in ZnO,[24] a large amount of electrons in the nanowire are compensated by Na-doping, which makes the nanowire more resistive and the good contact more difficult to obtain, although the Na-doped ZnO nanowire is still n-type under the growth conditions in this experiment, as shown in Fig. S6.† At the same time Ag can also be utilized as a p-type dopant in ZnO nanowires[25] besides forming a nanoisland chain on the surface. During the voltage sweeping from 0 V to 40 V, Ag atoms doped into the nanowire moved towards the grounded side. The biased side was more conductive while the grounded side was more resistive. Finally, a good contact between the nanowire and Ag at the biased side was formed while that at the grounded side kept as a Schottky contact. The whole nanowire system can be treated as a resistor in series to a Schottky diode, as shown in the inset of Fig. 3(a).

In summary, current self-complianced and self-rectifying bipolar resistive switching was observed in Ag-contacted, Na-doped ZnO nanowire resistive memory. SEM, HSR-AES and *I–V* characteristics show that the resistive switching was controlled by the formation and rupture of the Ag nano-island chain on the surface of the nanowire. The self-compliance is induced by Na-doping and partial retraction of Ag from the nanoisland chain while the self-rectifying behavior mainly originates from the asymmetric contact between the nanowire and Ag contact induced by Na-doping and Ag atom segregation and doping. The demonstration of current self-compliance and self-rectification in Na-doped nanowire resistive memory can significantly simplify the future resistive random access memory circuitry because no separate selector device is necessary.

The authors acknowledge the financial and program support of the Microelectronics Advanced Research Corporation (MARCO) and its Focus Center on Function Engineered Nano Architectonics (FENA), the DARPA/Defense Microelectronics Activity (DMEA) under agreement number H94003-10-2-1003 (3D Electronics), and National Natural Science Foundation of China (no. 50902065). We thank the Applied Technology Training Center at San Bernardino Community College District for the AFM equipment. Prof. Jing Qi and Mr Jian Huang had equal contribution to this work.

Notes and references

1 A. Asamitsu, Y. Tomioka, H. Kuwahara and Y. Tokura, *Nature*, 1997, **388**, 50–52.
2 R. Waser and M. Aono, *Nat. Mater.*, 2007, **6**, 833–840.
3 M. J. Lee, Y. Park, D. S. Suh, E. H. Lee, S. Seo, D. C. Kim, R. Jung, B. S. Kang, S. E. Ahn, C.-B. Lee, D. H. Seo, Y. K. Cha, I. K. Yoo, J. S. Kim and B. H. Park, *Adv. Mater.*, 2007, **19**, 3919–3923.
4 C. Moreno, C. Munuera, S. Valencia, F. Kronast, X. Obradors and C. Ocal, *Nano Lett.*, 2010, **10**, 3828–3835.
5 J. Borghetti, G. S. Snider, P. J. Kuekes, J. J. Yang, D. R. Stewart and R. S. Williams, *Nature*, 2010, **464**, 873–876.
6 Q. Xia, W. Robinett, M. W. Cumbie, N. Banerjee, T. J. Cardinali, J. J. Yang, W. Wu, X. Li, W. M. Tong, D. B. Strukov, G. S. Snider, G. Medeiros-Ribeiro and R. S. Williams, *Nano Lett.*, 2009, **9**, 3640–3645.
7 L. O. Chua, *IEEE Trans. Circuit Theory*, 1971, **18**, 507–519.
8 L. O. Chua and S. M. Kang, *Proc. IEEE*, 1976, **64**, 209–223.
9 D. B. Strukov, G. S. Sinder, D. R. Stewart and R. S. Williams, *Nature*, 2008, **453**, 80–83.
10 Y. V. Pershin and M. Di Ventra, *IEEE Trans. Circuits Syst. I, Reg. Papers*, 2010, **57**, 1857–1864.
11 K. K. Likharev, *J. Nanoelectron. Optoelectron.*, 2008, **3**, 203–230.

12 S. H. Jo, T. Chang, I. Ebong, B. B. Bhadviya, P. Mazumder and W. Lu, *Nano Lett.*, 2010, **10**, 1297–1301.
13 Y. V. Pershin and M. Di Ventra, *Neural Network*, 2010, **23**, 881–886.
14 Q. Zuo, S. Long, Q. Liu, S. Zhang, Q. Wang, Y. Li, Y. Wang and M. Liu, *J. Appl. Phys.*, 2009, **106**, 073724-1–073724-5.
15 Z. Wang, W. G. Zhu, A. Y. Du, L. Wu, Z. Fang, X. A. Tran, W. J. Liu, K. L. Zhang and H.-Y. Yu, *IEEE Trans. Electron Devices*, 2012, **59**, 1203–1208.
16 K. Kim, S. Gaba, D. Wheeler, J. M. Cruz-Albrecht, T. Hussain, N. Srinivasa and W. Lu, *Nano Lett.*, 2012, **12**, 389–395.
17 Y. Yang, X. Zhang, M. Gao, F. Zeng, W. Zhou, S. Xie and F. Pan, *Nanoscale*, 2011, **3**, 1917–1921.
18 Y. Yang, P. Gao, S. Gaba, T. Chang, X. Pan and W. Lu, *Nat. Comm.*, 2012, **3**, 732-1–732-8.
19 L. C. Bum, L. D. Soo, A. Benayad, L. S. Ryul, C. Man, L. Myoung-Jae, H. Jihyum, K. C. Jung and U. I. Chung, *IEEE Electron Device Lett.*, 2011, **32**, 399–401.
20 K. Kim, S. Jo, S. Gaba and W. Lu, *Appl. Phys. Lett.*, 2010, **96**, 053106-1–053106-3.
21 S. Bayan and D. Mohanta, *J. Electron. Mater.*, 2012, **41**, 1955–1961.
22 O. Harnack, C. Pacholski, H. Weller, A. Yasuda and J. M. Wessels, *Nano Lett.*, 2003, **3**, 1097–1101.
23 C. S. Lao, J. Liu, P. Gao, L. Zhang, D. Davidovic, R. Tummala and Z. L. Wang, *Nano Lett.*, 2006, **6**, 263–266.
24 W. Liu, F. Xiu, K. Sun, Y. Xie, K. L. Wang, J. Zou, Z. Yang and J. Liu, *J. Am. Chem. Soc.*, 2010, **132**, 2498–2499.
25 I. S. Kim, E. K. Jeong, D. Y. Kim, M. Kumar and S. Y. Choi, *Appl. Surf. Sci.*, 2009, **255**, 4011.

 This journal is © The Royal Society of Chemistry 2013